CARITAS UNIVERSITY AMORJI-NIKE, EMENE, ENUGU STATE
Caritas Journal of Engineering Technology
CJET, Volume 4, Issue 1 (2025)
Article's History: Received:20th December, 2024 Revised:27th January, 2025 Accepted: 21st February, 2025.

Voltage Stability Compensation in Electronics –Saturated Network Using Unified Power Flow Controller

Ifeagwu E.N
Department of Electrical and Electronic Engineering,
Federal University Otuoke, Bayelsa State,
ifeagwuen@fuotuoke.edu.ng

Ezema D.C.
Department of Electrical and Electronic Engineering,
State University of Medical and Applied Sciences (SUMAS), Igbo Eno, Enugu State, Nigeria.
donatus.ezema@sumas.edu.ng,

Abstract

Voltage stability is a critical aspect of power system operation, especially in networks with a high penetration of power electronic loads such as variable speed drives, converters, and renewable energy systems. These electronics-saturated networks often experience voltage fluctuations, harmonic distortions, and reactive power imbalances, which can lead to instability and reduced power quality. The Unified Power Flow Controller (UPFC), a key Flexible AC Transmission System (FACTS) device, offers a comprehensive solution to these challenges by providing simultaneous control of voltage, impedance, and phase angle in the transmission line. This paper presents an approach for voltage stability compensation in electronics-saturated networks using the UPFC. The shunt converter of the UPFC provides reactive power support, maintaining bus voltage levels and mitigating voltage sags caused by nonlinear electronic loads. Simultaneously, the series converter regulates line impedance and power flow, reducing line losses and improving load distribution. Additionally, the coordinated control of the shunt and series converters helps damp power oscillations and improve system resilience against sudden load variations. Advanced control strategies such as Proportional-Integral (PI) controllers, Fuzzy Logic Controllers (FLC), and Model Predictive Control (MPC) are discussed for optimizing the UPFC's performance under varying load conditions. Simulation results demonstrate that the UPFC significantly enhances voltage stability, reduces harmonic distortion, and improves overall power quality in an electronics-saturated network. The proposed solution is suitable for applications in modern power grids, including industrial plants, electric vehicle charging stations, and smart grid environments.

Keywords: Active power, reactive power, Unified Power flow Controller, FACT, STATCOM.

1.0 Introduction

Voltage stability is a crucial aspect of power system performance, ensuring reliable and continuous electricity delivery under varying load conditions (Mohanty et al., 2023). In modern power networks, the increasing use of power electronic devices, such as variable frequency drives, rectifiers, inverters, and renewable energy converters, has led to the emergence of electronics-saturated networks (Gaurav and Saxena, 2018). These networks are characterized by nonlinear and dynamic loads that can cause rapid voltage fluctuations, harmonic

distortions, and reactive power imbalances, resulting in voltage instability and power quality issues (Lakshmi et al., 2015). The challenges posed by electronics-saturated networks include: voltage sags and swells caused by sudden changes in load or supply conditions, harmonic distortions resulting from the switching operations of power electronic devices. reactive power imbalance due to the inductive and capacitive nature of electronic loads, power oscillations arising from uncoordinated power transfers (Mathad et al., 2018).

To address these challenges, Flexible AC Transmission System (FACTS) devices are widely used to enhance power system stability and control (Rai 2018). Among various FACTS devices, the Unified Power Flow Controller (UPFC) is the most comprehensive solution, as it can control multiple power system parameters simultaneously, including voltage, line impedance, and phase angle (Soruban et al., 2020). The UPFC integrates a shunt converter (STATCOM) and a series converter (SSSC) through a common DC link, providing both reactive power compensation and power flow control (Khonde et al., 2020).

In electronics-saturated networks, the UPFC plays a critical role in maintaining bus voltage by providing reactive power support through the shunt converter, regulating power flow by adjusting line impedance and controlling the phase angle through the series converter, mitigating harmonics by improving power factor and damping power oscillations, enhancing system stability by responding rapidly to load variations from electronic devices (Asha et al., 2021) .This paper focuses on the application of UPFC for voltage stability compensation in electronics-saturated networks. It explores the working principle of UPFC, control strategies for efficient operation, and the impact of the device on power quality and system stability (Bhowmik and Nandi, 2019). Additionally, simulation results are presented to demonstrate the effectiveness of UPFC in mitigating voltage instability and enhancing the reliability of power delivery in modern power systems. The paper aims to provide insights into the potential of UPFC technology for addressing voltage stability challenges in electronically dominated grids, which are increasingly prevalent in smart grids, industrial plants, and renewable energy integration systems. Power electronics is a proven technology that has transformed every facet of the electrical power network, impacting not only the distribution, utilization, and transmission of AC power but also the transmission of high voltage direct current (HVDC) (Jiang, 2010).

In order to achieve electronic controllability, the Flexible AC Transmission Systems (FACTS) concept makes considerable use of power electronic devices on the high-voltage side of the network. Electric Power Research Institute (EPRI) introduced FACTS in the 1980s; it capitalizes on advances in high-voltage and high-current power electronics . Both steady-state and transient performance are improved by this method, which also improves control over power flows in the high-voltage section of the network. The design and construction of power plant equipment, as well as the planning and management of transmission and distribution networks, are being affected by the shift to electronic controllability. Because they allow for quick control over energy flow pathways, these advances are predicted to completely transform energy transactions. FACTS has garnered substantial backing from electrical equipment makers, utilities, and research institutions worldwide, owing to its noteworthy economic and technological advantages. Globally, a variety of FACTS controllers have been put into practice, each with a specific purpose in mind to maximize power system efficiency and operation: load tap changers, phase-angle regulators, static VAR compensators, thyristor-controlled series compensators, interphase power controllers, static compensators, and unified power flow controllers (Zhang et al., 2018).
FACTS devices introduce a wide operational range to increase the thermal limits of a power system and improve its stability. FACTS devices have been used for: active and reactive power control, voltage control stability and sub synchronous resonance mitigation, power oscillation damping, transients and dynamics stability, fault current limiting, flicker mitigation, power system security enhancement.

2.0 Materials and Method

2.1 Materials

The materials used in this paper include:

(I) UPFC : This consists of a series and shunt converter connected through a common link
(II) Power Supply: Three –phase AC power source

(III) Transmission Line Model: This represents the saturated network
(IV) Power Transformers : This is for voltage regulation
(V) Voltage and Current Sensors
(VI) Microcontroller/Controller: This include the Digital Signal Processor for real time control
(VII) Software Tools: MATLAB/Simulink for simulation and analysis
(VIII) Measurement Instrument: Multimeters, Oscilloscope and power analyzers for performance evaluation.

2.2 Method

UPFC was installed in the correct places for the system to have higher voltage stability. The weak busses in the system were identified by a load flow analysis, which helped select the ideal position. The Newton Raphson method was used to analyse the load flow since it is very effective due to its robust convergence properties. It was used in this paper to ascertain the steady state voltages at each of the system's busses

2.2.1 UPFC Placement and Configuration

This section examines the modeling and simulation techniques utilized for the power system network as well as the UPFC models that regulate the system's bus voltages. It also provides a thorough mathematical representation of the simulations' used solutions. The One-line diagram of the power system used as the model for this paper is shown in Figure 1 .

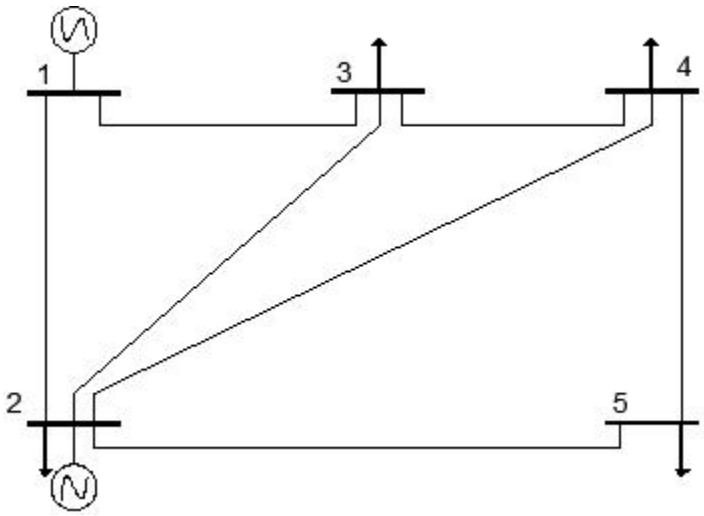

Figure 1: One line diagram of the power system model

2.2.2 Newton Raphson Load Flow Method

This approach uses iteration to solve the following set of nonlinear algebraic equations (Gopinath et al., 2014).

$$\left.\begin{aligned} f_1(x_1, x_2, \cdots, x_N) &= 0, \\ f_2(x_1, x_2, \cdots, x_N) &= 0, \\ &\vdots \\ f_N(x_1, x_2, \cdots, x_N) &= 0, \end{aligned}\right\}, \quad \text{or} \quad \mathbf{F(X)} = \mathbf{0} \tag{1}$$

where F represents the set of 'n' nonlinear equations, and X is the vector of 'n' unknown state variables.
The determination of the vector of state variables X was done by performing a Taylor series expansion of F(X) about an initial estimate X (^{0}):

$$\boldsymbol{F(X) = F\left(X^{(0)}\right) + J\left(X^{(0)}\right)\left(X - X^{(0)}\right) + \text{higher-order terms}} \tag{2}$$

where J(X (^{0})) is a matrix of first-order partial derivatives of F(X) with respect to X,

termed the Jacobian, evaluated at X=X (^{0}).

This expansion lends itself to a suitable formulation for calculating the vector of state variables X by that X (^{1}) is the value computed by the algorithm at iteration 1 and that this value is sufficiently close to the initial estimate X (^{0}). Neglecting all high-order derivative terms in equation (2) we obtain equation (3)

$$\underbrace{\begin{bmatrix} f_{1(X^{(1)})} \\ f_{2(X^{(1)})} \\ \vdots \\ f_{n(X^{(1)})} \end{bmatrix}}_{F(X^{(1)})} \approx \underbrace{\begin{bmatrix} f_{1(X^{(0)})} \\ f_{2(X^{(0)})} \\ \vdots \\ f_{n(X^{(0)})} \end{bmatrix}}_{F(X^{(0)})} + \underbrace{\begin{bmatrix} \frac{\partial f_1(X)}{\partial x_1} & \frac{\partial f_1(X)}{\partial x_2} & \cdots & \frac{\partial f_1(X)}{\partial x_n} \\ \frac{\partial f_2(X)}{\partial x_1} & \frac{\partial f_2(X)}{\partial x_2} & \cdots & \frac{\partial f_2(X)}{\partial x_n} \\ \vdots & \vdots & \ddots & \vdots \\ \frac{\partial f_n(X)}{\partial x_1} & \frac{\partial f_n(X)}{\partial x_2} & \cdots & \frac{\partial f_n(X)}{\partial x_n} \end{bmatrix}}_{J(X^{(0)})} \underbrace{\begin{bmatrix} X_1^{(1)} - X_1^{(0)} \\ X_2^{(1)} - X_2^{(0)} \\ \vdots \\ X_n^{(n)} - X_n^{(0)} \end{bmatrix}}_{X^{(1)} - X^{(0)}} \quad (3)$$

Generalisin, the equation (3) for the case of iteration (i),

$$\boldsymbol{F(X^{(i)}) \approx F(X^{(i-1)}) + J(X^{(i-1)})(X^{(i)} - X^{(i-1)})} \quad (4)$$

where i = 1, 2 . . . .

Assuming that X(^{i}) is sufficiently close to the solution X(*), then FX(^{i}) ≈ FX(*) = 0. Thus, equation (4) becomes

$$\boldsymbol{F(X^{(i-1)}) + J(X^{(i-1)})(X^{(i)} - X^{(i-1)}) = 0} \quad (5)$$

and solving for X(^{i}),

$$\boldsymbol{X^{(i)} = X^{(i-1)} - J^{-1}(X^{(i-1)})F(X^{(i-1)})} \quad (6)$$

The iterative solution can be expressed as a function of the correction vector

ΔX(^{i})= X(^{i}) - X($^{i-1}$),

$$\boldsymbol{\Delta X^{(i)} = -J^{-1}(X^{(i-1)})F(X^{(i-1)})} \quad (7)$$

and the initial estimates are updated using the following relation:

$$\boldsymbol{\Delta X^{(i)} = (X^{(i-1)}) + \Delta X^{(i)}} \quad (8)$$

The calculations are repeated as many times as required using the most up-to-date values of X in equation (8). This is done until the mismatches ΔX are within a prescribed small tolerance (i.e. 1e -12).

The essential equations must be represented in the form of Equation (8), where X is the set of unknown nodal voltage magnitudes and phase angles, in order to apply the Newton Raphson approach to the power flow problem (Sindekar and Parate, 2012) The power flow Newton Raphson algorithm can be described by the following connection since the power mismatch equations ΔP and ΔQ are enlarged around a base point (θ(0), V(0)) (Singh, 2020):

$$\underbrace{\begin{bmatrix} \Delta \mathbf{P} \\ \Delta \mathbf{Q} \end{bmatrix}^{(i)}}_{\mathbf{F}(\mathbf{X}^{(i-1)})} = -\underbrace{\begin{bmatrix} \frac{\partial \mathbf{P}}{\partial \boldsymbol{\theta}} & \frac{\partial \mathbf{P}}{\partial \mathbf{V}}\mathbf{V} \\ \frac{\partial \mathbf{Q}}{\partial \boldsymbol{\theta}} & \frac{\partial \mathbf{Q}}{\partial \mathbf{V}}\mathbf{V} \end{bmatrix}^{(i)}}_{\mathbf{J}(\mathbf{X}^{(i-1)})} \underbrace{\begin{bmatrix} \Delta \boldsymbol{\theta} \\ \frac{\Delta \mathbf{V}}{\mathbf{V}} \end{bmatrix}^{(i)}}_{\Delta \mathbf{X}^{(i)}} \quad (9)$$

The various matrices in the Jacobian may consists of up to (nb - 1) × (nb - 1) elements of the form:

$$\left.\begin{matrix} \frac{\partial P_k}{\partial \theta_m}, & \frac{\partial P_k}{\partial V_m} V_m, \\ \frac{\partial Q_k}{\partial \theta_m}, & \frac{\partial Q_k}{\partial V_m} V_m, \end{matrix}\right\} \quad (10)$$

where nb is the number of buses with the slack bus entries removed, and k and m are the values of 1,..., and nb, respectively. Removing, the rows and columns for PV buses that relate to reactive power and voltage magnitude are removed. Moreover, the matching k–m item in the Jacobian is null when buses k and m are not connected directly by a transmission element. Because real power networks have relatively modest levels of connectedness, power flow Jacobians are quite sparse. They have the trait of being symmetrical in structure but not in value.
Note that the correction terms ΔVm are divided by Vm in order to offset the multiplication of the Jacobian terms $(\partial PK/\partial Vm)Vm$ and $(\partial QK/\partial V_m)\ V_m$ by V_m. The derivative terms provided below demonstrate how this trick produces helpful calculations that can be made simpler.

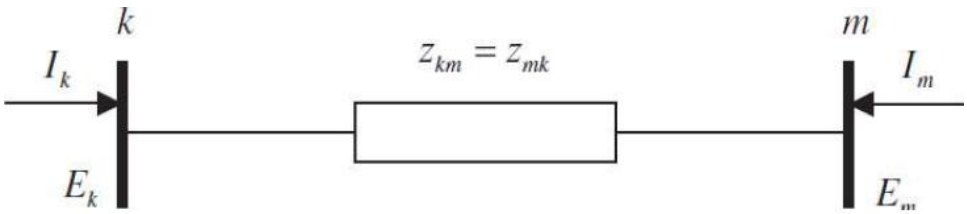

Figure 2: A two bus system for illustrating Newton Raphson Power flows (Vaibhav ,et al., 2013)

Consider the element connected between buses k and m in Figure 2, for which self and mutual Jacobian terms are given in section 3.2.1:

2.2.3 Formation of The Y-Bus

In order to develop suitable power flow equations, it is necessary to find relationships between injected bus currents and bus voltages. Based on Figure 2 the injected complex current at bus k, denoted by I_K, may be expressed in terms of the complex bus voltages E_k and E_m as follows:

$$I_k = \frac{1}{z_{km}}(E_k - E_m) = y_{km}(E_k - E_m) \tag{11}$$

Similarly for bus m,

$$I_m = \frac{1}{z_{mk}}(E_m - E_k) = y_{mk}(E_m - E_k) \tag{12}$$

The above equations can be written in matrix form as,

$$\begin{bmatrix} I_k \\ I_m \end{bmatrix} = \begin{bmatrix} y_{km} & -y_{km} \\ -y_{mk} & y_{mk} \end{bmatrix} \begin{bmatrix} E_k \\ E_m \end{bmatrix} \tag{13}$$

or

$$\begin{bmatrix} I_k \\ I_m \end{bmatrix} = \begin{bmatrix} Y_{kk} & Y_{km} \\ Y_{mk} & Y_{mm} \end{bmatrix} \begin{bmatrix} E_k \\ E_m \end{bmatrix} \tag{14}$$

where the bus admittances and voltages can be expressed in more explicit form:

$$Y_{ij} = G_{ij} + \mathrm{j}\,B_{ij} \tag{15}$$

$$E_i = V_i e^{\mathrm{j}\theta_i} = V_i(\cos\theta_i + \mathrm{j}\sin\theta_i) \tag{16}$$

where i = k, m; j = k, m
The complex power injected at bus k consists of an active and a reactive component and may be expressed as a function of the nodal voltage and the injected current at the bus:

$$S_k = P_k + \mathrm{j}\,Q_k = E_k\,I_k^* = E_k\,(Y_{kk}\,E_k + Y_{km}\,E_m)^* \quad (17)$$

where I_K is the complex conjugate of the current injected at bus k.
The expressions for P_k^{cal} and Q_k^{cal} can be determined by substituting equations 15 and 16 into equation 17, and separating into real and imaginary parts, we arrive at equation (18)

$$P_k^{\mathrm{cal}} = V_k^2\,G_{kk} + V_k\,V_m\,[G_{km}\cos(\theta_k - \theta_m) + B_{km}\sin(\theta_k - \theta_m)] \quad (18)$$

$$Q_k^{\mathrm{cal}} = -V_k^2\,B_{kk} + V_k\,V_m\,[G_{km}\sin(\theta_k - \theta_m) - B_{km}\cos(\theta_k - \theta_m)] \quad (19)$$

Equations (18) and (19) are the two important power flow equations and are used in deriving the Jacobian matrix.

2.2.4. Forming The Jacobian Matrix

For k ≠ m,

$$\frac{\partial P_{k,l}}{\partial \theta_{m,l}} = V_k\,V_m\,[G_{km}\sin(\theta_k - \theta_m) - B_{km}\cos(\theta_k - \theta_m)] \quad (20)$$

$$\frac{\partial P_{k,l}}{\partial V_{m,l}} V_{m,l} = V_k\,V_m\,[G_{km}\cos(\theta_k - \theta_m) + B_{km}\sin(\theta_k - \theta_m)] \quad (21)$$

$$\frac{\partial Q_{k,l}}{\partial \theta_{m,l}} = -\frac{\partial P_{k,l}}{\partial V_{m,l}} V_{m,l} \quad (22)$$

$$\frac{\partial Q_{k,l}}{\partial V_{m,l}} V_{m,l} = \frac{\partial P_{k,l}}{\partial \theta_{m,l}} \quad (23)$$

For K = m,

$$\frac{\partial P_{k,l}}{\partial \theta_{k,l}} = -Q_k^{\mathrm{cal}} - V_k^2 B_{kk} \quad (24)$$

$$\frac{\partial P_{k,l}}{\partial V_{k,l}} V_{k,l} = P_k^{\mathrm{cal}} + V_k^2 G_{kk} \quad (25)$$

$$\frac{\partial Q_{k,l}}{\partial \theta_{k,l}} = P_k^{\mathrm{cal}} - V_k^2 G_{kk} \quad (26)$$

3.2.5 Incorporating the UPFC in Newton Raphson Load Flow

Figure 3 : shows unified power flow controller equivalent circuit

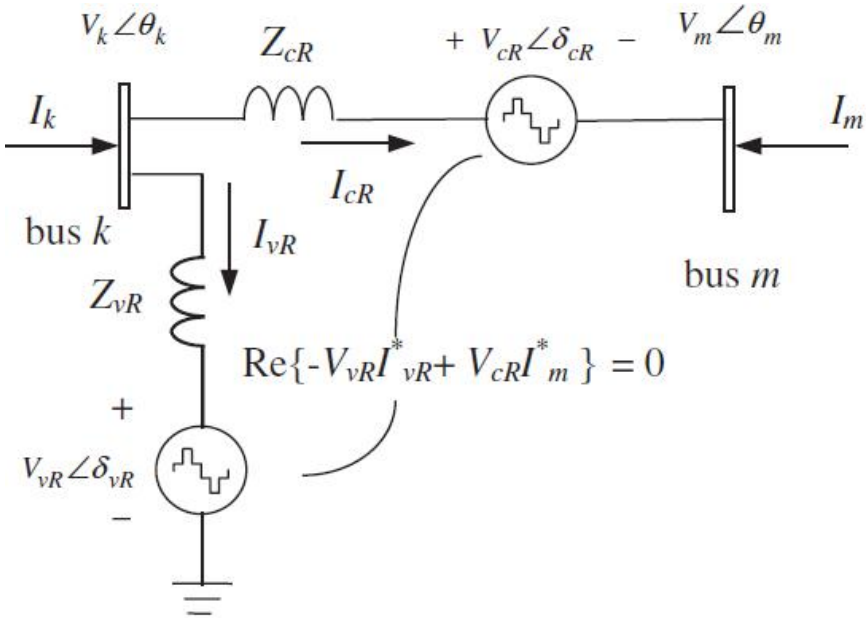

Figure 3 : Unified power flow controller equivalent circuit

The UPFC voltage sources are:

$$E_{vR} = V_{vR}(\cos\ \delta_{vR} + \mathrm{j}\sin\delta_{vR}) \quad (27)$$

$$E_{cR} = V_{cR}(\cos\delta_{cR} + \mathrm{j}\sin\delta_{cR}) \quad (28)$$

where $V_{vR}$and δ_{vR} are the controllable magnitude ($V_{vR\,min} \le V_{vR} \le V_{vR\,max}$) and phase angle ($0 \le \delta_{vR} \le 2\pi$) of the voltage source representing the shunt converter. The magnitude V_{cR} and phase angle δ_{cR} of the voltage source representing the series converter are controlled between limits ($V_{vR\,min} \le V_{vR} \le V_{vR\,max}$) and ($0 \le \delta_{vR} \le 2\pi$), respectively.

The phase angle of the series-injected voltage determines the mode of power flow control. If δ_{cR} is in phase with the nodal voltage angleθ_k, the UPFC regulates the terminal voltage. If δ_{cR} is in quadature with respect to θ_k, it controls active power flow, acting as a phase shifter. If δ_{cR} is in quadrature with the line current angle then it controls active power flow, acting as a variable series compensator. At any other value of δ_{cR}, the UPFC operates as a combination of voltage regulator, variable series compensator, and phase shifter. The magnitude of the series-injected voltage determines the amount of power flow to be controlled.

From Figure 3 and equations (18) and (19), the active and reactive power equations at bus k are:

$$\begin{aligned} P_k = {} & V_k^2 G_{kk} + V_k V_m[G_{km}\cos(\theta_k - \theta_m) + B_{km}\sin(\theta_k - \theta_m)] \\ & + V_k V_{cR}[G_{km}\cos(\theta_k - \delta_{cR}) + B_{km}\sin(\theta_k - \delta_{cR})] \\ & + V_k V_{vR}[G_{vR}\cos(\theta_k - \delta_{vR}) + B_{vR}\sin(\theta_k - \delta_{vR})], \end{aligned} \quad (29)$$

$$\begin{aligned} Q_k = {} & -V_k^2 B_{kk} + V_k V_m[G_{km}\sin(\theta_k - \theta_m) - B_{km}\cos(\theta_k - \theta_m)] \\ & + V_k V_{cR}[G_{km}\sin(\theta_k - \delta_{cR}) - B_{km}\cos(\theta_k - \delta_{cR})] \\ & + V_k V_{vR}[G_{vR}\sin(\theta_k - \delta_{vR}) - B_{vR}\cos(\theta_k - \delta_{vR})]; \end{aligned} \quad (30)$$

at bus m:

$$\begin{aligned} P_m = {} & V_m^2 G_{mm} + V_m V_k[G_{mk}\cos(\theta_m - \theta_k) + B_{mk}\sin(\theta_m - \theta_k)] \\ & + V_m V_{cR}[G_{mm}\cos(\theta_m - \delta_{cR}) + B_{mm}\sin(\theta_m - \delta_{cR})], \end{aligned} \quad (31)$$

$$Q_m = -V_m^2 B_{mm} + V_m V_k [G_{mk} \sin(\theta_m - \theta_k) - B_{mk} \cos(\theta_m - \theta_k)] + V_m V_{cR} [G_{mm} \sin(\theta_m - \delta_{cR}) - B_{mm} \cos(\theta_m - \delta_{cR})]; \quad (32)$$

Series converter:

$$P_{cR} = V_{cR}^2 G_{mm} + V_{cR} V_k [G_{km} \cos(\delta_{cR} - \theta_k) + B_{km} \sin(\delta_{cR} - \theta_k)] + V_{cR} V_m [G_{mm} \cos(\delta_{cR} - \theta_m) + B_{mm} \sin(\delta_{cR} - \theta_m)], \quad (33)$$

$$Q_{cR} = -V_{cR}^2 B_{mm} + V_{cR} V_k [G_{km} \sin(\delta_{cR} - \theta_k) - B_{km} \cos(\delta_{cR} - \theta_k)] + V_{cR} V_m [G_{mm} \sin(\delta_{cR} - \theta_m) - B_{mm} \cos(\delta_{cR} - \theta_m)]; \quad (34)$$

Shunt converter:

$$P_{vR} = -V_{vR}^2 G_{vR} + V_{vR} V_k [G_{vR} \cos(\delta_{vR} - \theta_k) + B_{vR} \sin(\delta_{vR} - \theta_k)] \quad (35)$$

$$Q_{vR} = V_{vR}^2 B_{vR} + V_{vR} V_k [G_{vR} \sin(\delta_{vR} - \theta_k) - B_{vR} \cos(\delta_{vR} - \theta_k)] \quad (36)$$

Assuming loss-less converter valves, the active power supplied to the shunt converter, P_{vR}, equals the active power demanded by the series converter, P_{cR}; that is,

$$P_{vR} + P_{cR} = 0\ 9 \quad (37)$$

In a coupling transformers with no resistance, the active power at bus k matches the active power at bus m. Then,

$$P_{vR} + P_{cR} = P_k + P_m = 0 \quad (38)$$

The UPFC power equations, in linearized form, are combined with those of the AC network. For the case when the UPFC controls the following parameters: (1) voltage magnitude at the shunt converter terminal (bus k), (2) active power flow from bus m to bus k, and (3) reactive power injected at bus m, and taking bus m to be a PQ bus, the linearized system of equations is as follows:

$$\begin{bmatrix} \Delta P_k \\ \Delta P_m \\ \Delta Q_k \\ \Delta Q_m \\ \Delta P_{mk} \\ \Delta Q_{mk} \\ \Delta P_{bb} \end{bmatrix} = \begin{bmatrix} \frac{\partial P_k}{\partial \theta_k} & \frac{\partial P_k}{\partial \theta_m} & \frac{\partial P_k}{\partial V_{vR}} V_{vR} & \frac{\partial P_k}{\partial V_m} V_m & \frac{\partial P_k}{\partial \delta_{cR}} & \frac{\partial P_k}{\partial V_{cR}} V_{cR} & \frac{\partial P_k}{\partial \delta_{vR}} \\ \frac{\partial P_m}{\partial \theta_k} & \frac{\partial P_m}{\partial \theta_m} & 0 & \frac{\partial P_m}{\partial V_m} V_m & \frac{\partial P_m}{\partial \delta_{cR}} & \frac{\partial P_m}{\partial V_{cR}} V_{cR} & 0 \\ \frac{\partial Q_k}{\partial \theta_k} & \frac{\partial Q_k}{\partial \theta_m} & \frac{\partial Q_k}{\partial V_{vR}} V_{vR} & \frac{\partial Q_k}{\partial V_m} V_m & \frac{\partial Q_k}{\partial \delta_{cR}} & \frac{\partial Q_k}{\partial V_{cR}} V_{cR} & \frac{\partial Q_k}{\partial \delta_{vR}} \\ \frac{\partial Q_m}{\partial \theta_k} & \frac{\partial Q_m}{\partial \theta_m} & 0 & \frac{\partial Q_m}{\partial V_m} V_m & \frac{\partial Q_m}{\partial \delta_{cR}} & \frac{\partial Q_m}{\partial V_{cR}} V_{cR} & 0 \\ \frac{\partial P_{mk}}{\partial \theta_k} & \frac{\partial P_{mk}}{\partial \theta_m} & 0 & \frac{\partial P_{mk}}{\partial V_m} V_m & \frac{\partial P_{mk}}{\partial \delta_{cR}} & \frac{\partial P_{mk}}{\partial V_{cR}} V_{cR} & 0 \\ \frac{\partial Q_{mk}}{\partial \theta_k} & \frac{\partial Q_{mk}}{\partial \theta_m} & 0 & \frac{\partial Q_{mk}}{\partial V_m} V_m & \frac{\partial Q_{mk}}{\partial \delta_{cR}} & \frac{\partial Q_{mk}}{\partial V_{cR}} V_{cR} & 0 \\ \frac{\partial P_{bb}}{\partial \theta_k} & \frac{\partial P_{bb}}{\partial \theta_m} & \frac{\partial P_{bb}}{\partial V_{vR}} V_{vR} & \frac{\partial P_{bb}}{\partial V_m} V_m & \frac{\partial P_{bb}}{\partial \delta_{cR}} & \frac{\partial P_{bb}}{\partial V_{cR}} V_{cR} & \frac{\partial P_{bb}}{\partial \delta_{vR}} \end{bmatrix} \begin{bmatrix} \Delta\theta_k \\ \Delta\theta_m \\ \frac{\Delta V_{vR}}{V_{vR}} \\ \frac{\Delta V_m}{V_m} \\ \Delta\delta_{cR} \\ \frac{\Delta V_{cR}}{V_{cR}} \\ \Delta\delta_{vR} \end{bmatrix} \quad (39)$$

The MATLAB script implementing the above Newton-Raphson load flow and the incorporation of the UPLC equations is given in section 3.2.3

2.2.6 MATLAB script Implementation

```
% THE PROGRAM WITHOUT UPFC
PowerFlowsData; %Function to read network data
[YR,YI] = YBus(tlsend,tlrec,tlresis,tlreac,tlsuscep,...
tlcond,shbus,shresis,shreac,ntl,nbb,nsh); %Function to calculate the Ybus
% GENERAL SETTINGS
D = zeros(1,nmax);
flag = 0;
it = 1;
% CALCULATE NET POWERS
[PNET,QNET] = NetPowers(nbb,ngn,nld,genbus,loadbus,PGEN,QGEN,...
PLOAD,QLOAD);
while( it<itmax&& flag==0 )
% CALCULATED POWERS
[PCAL,QCAL] = CalculatedPowers(nbb,VM,VA,YR,YI);
% CHECK FOR POSSIBLE GENERATOR'S REACTIVE POWERS LIMITS VIOLATIONS
[QNET,bustype] = GeneratorsLimits(ngn,genbus,bustype,QGEN,QMAX,...
QMIN,QCAL,QNET, QLOAD, it, VM, nld, loadbus);
% POWER MISMATCHES
[DPQ,DP,DQ,flag] = PowerMismatches(nmax,nbb,tol,bustype,flag,PNET,...
QNET,PCAL,QCAL);
% JACOBIAN FORMATION

[JAC] = NewtonRaphsonJacobian(nmax,nbb,bustype,PCAL,QCAL,VM,VA,...
YR,YI);
% SOLVE FOR THE STATE VARIABLES VECTOR
D = JAC\DPQ';
% UPDATE STATE VARIABLES
[VA,VM] = StateVariablesUpdates(nbb,D,VA,VM);
it = it + 1;
end
[PQsend,PQrec,PQloss,PQbus] = PQflows(nbb,ngn,ntl,nld,...
genbus,loadbus,tlsend,tlrec,tlresis,tlreac,tlcond,tlsuscep,PLOAD,...
QLOAD,VM,VA);
Psend=real(PQsend*100)';
Prec=real(PQrec*100)';
Ploss=real(PQloss*100)';
Qsend=imag(PQsend*100)';
Qrec=imag(PQrec*100)';
Qloss=imag(PQloss*100)';
PQbus=(PQbus*100)';
% End function Newton-Raphson
% Results
VA=VA*180/pi; %Nodal voltage phase angles (deg)
disp(['bus voltage in pu          ','voltage angle in degree'])
SM = [VM;VA];
% - - - Main UPFC Program
PowerFlowsData; %Function to read network data
UPFCdata; %Function to read the UPFC data
[YR,YI] = YBus(tlsend,tlrec,tlresis,tlreac,tlsuscep,...
tlcond,shbus,shresis,shreac,ntl,nbb,nsh); %Function to calculate the Ybus
% GENERAL SETTING
D = zeros(1,nmax);
flag = 0;
it = 1;
% CALCULATE NET POWERS
[PNET,QNET] = NetPowers(nbb,ngn,nld,genbus,loadbus,PGEN,QGEN,...
PLOAD,QLOAD);
while( it<itmax&& flag==0 )
```

```
% CALCULATED POWERS
[PCAL,QCAL] = CalculatedPowers(nbb,VM,VA,YR,YI);
% CHECK FOR POSSIBLE GENERATOR'S REACTIVE POWERS LIMITS VIOLATIONS
[QNET,bustype] = GeneratorsLimits(ngn,genbus,bustype,QGEN,QMAX,...
QMIN,QCAL,QNET, QLOAD, it, VM, nld, loadbus);
% UPFC CALCULATED POWER
[PspQsend,PspQrec,PQcr,PQvr,PCAL,QCAL] = UPFCCalpower...
(nbb,VA, VM,NUPFC,UPFCsend,UPFCrec,Xcr,Xvr,Vcr,Tcr,Vvr,Tvr,PCAL,...
QCAL);

% POWER MISMATCHES
[DPQ,DP,DQ,flag] = PowerMismatches(nmax,nbb,tol,bustype,flag,PNET,...
QNET,PCAL,QCAL);
% UPFC POWER MISMATCHES
[DPQ,flag] = UPFCPowerMismatches(flag,tol,nbb,DPQ,VM,VA,NUPFC,Flow,...
Psp,PSta,Qsp,QSta,PspQsend,PspQrec,PQcr,PQvr);
if flag == 1
break
end
% JACOBIAN FORMATION
[JAC] = NewtonRaphsonJacobian(nmax,nbb,bustype,PCAL,QCAL,...
VM,VA,YR,YI);
% MODIFICATION OF THE JACOBIAN FOR UPFC
[JAC] = UPFCJacobian(nbb,JAC,VM,VA,NUPFC,UPFCsend,...
UPFCrec,Xcr,Xvr,Flow,PSta,QSta,Vcr,Tcr,Vvr,Tvr,VvrSta);
% SOLVE JOCOBIAN
D = JAC\DPQ';
% UPDATE THE STATE VARIABLES VALUES
[VA,VM] = StateVariablesUpdates(nbb,D,VA,VM);
% UPDATE THE TCSC VARIABLES
[VM,Vcr,Tcr,Vvr,Tvr] = UPFCUpdating(nbb,VM,D,NUPFC,UPFCsend,PSta,...
QSta,Vcr,Tcr,Vvr,Tvr,VvrTar,VvrSta);
%CHECK VOLTAGE LIMITS IN THE CONVERTERS
[Vcr,Vvr] = UPFCLimits(NUPFC,Vcr,VcrLo,VcrHi,Vvr,VvrLo,VvrHi);
it = it + 1;
end
%Function to calculate the power flows in the UPFC controller
 [UPFC_PQsend,UPFC_PQrec,PQcr,PQvr] = PQUPFCpower(nbb,...
VA,VM, NUPFC,UPFCsend,UPFCrec,Xcr,Xvr,Vcr,Tcr,Vvr,Tvr);
 [PQsend,PQrec,PQloss,PQbus] = PQflows(nbb,ngn,ntl,nld,genbus,...
loadbus,tlsend,tlrec,tlresis,tlreac,tlcond,tlsuscep,PLOAD,QLOAD,...
VM,VA);
Psend=real(PQsend*100)';
Prec=real(PQrec*100)';
Ploss=real(PQloss*100)';
Qsend=imag(PQsend*100)';
Qrec=imag(PQrec*100)';
Qloss=imag(PQloss*100)';
PQbus=(PQbus*100)';
% End of UPFC main program
%Print results
it; %Number of iterations
VA=VA*180/pi; %Nodal voltage phase angles (deg)
disp(['bus voltage in pu           ','voltage angle in degree'])
SM = [VM;VA];
fprintf('%15.4f %23.4f\n',SM)
```

3.0 Results and Discussion

3.1 Results

The results obtained from the simulations are shown in Table 1. Figure 4 shows Voltages of the buses without the UPFC between buses 3 and 4. Table 2 shows the line flows and losses Without UPFC. Figure 5 shows voltages of the buses with the UPFC between buses 3 and 4 while Figure 6 shows voltages of the buses with and without the UPFC between buses 3 and 4. Table 6 shows Bus Data: IEEE 5 Bus System while Table 7 shows the Line Data for IEEE 5 Bus.

3.1.1 Case 1: Newton-Raphson load flow carried out without the UPFC, considered as the normal condition. This result is depicted in Tables 1 and 2.

Table 1: Bus Voltages Without the UPFC

Bus voltage in pu	Voltage angle in degree
1.0600	0.0000
1.0000	-2.0612
0.9872	-4.6367
0.9841	-4.9570
0.9717	-5.7649

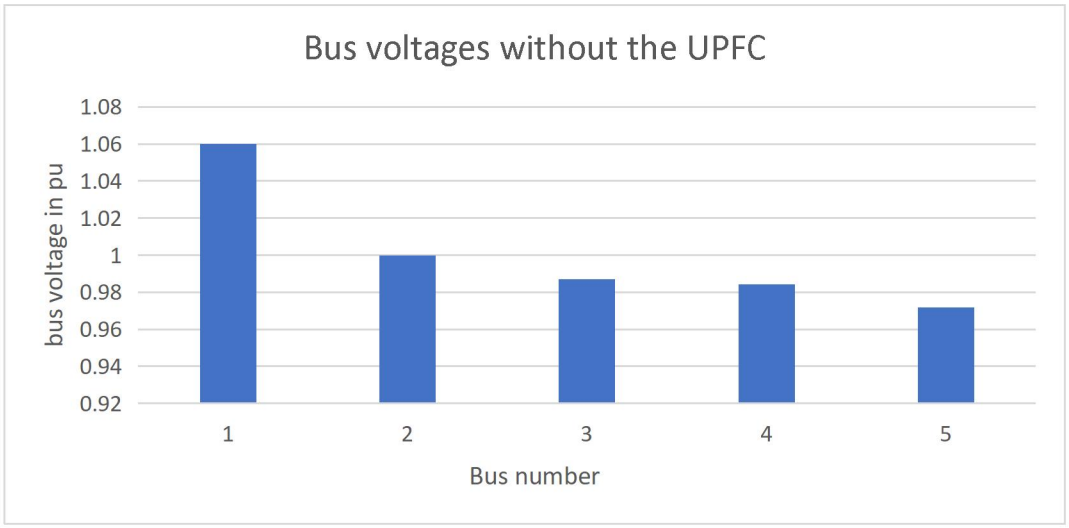

Figure 4: Voltages of the buses without the UPFC between buses 3 and 4

Table 2.Line Flows and Losses Without UPFC

Line FLow and Losses

From Bus	To Bus	P MW	Q MVar	From Bus	To Bus	P MW	Q MVar	Line Loss MW	Line Loss MVar
1	2	89.331	73.995	2	1	-86.846	-72.908	2.486	1.087
1	3	41.791	16.820	3	1	-40.273	-17.513	1.518	-0.692
2	3	24.473	-2.518	3	2	-24.113	-0.352	0.360	-2.871
2	4	27.713	-1.724	4	2	-27.252	-0.831	0.461	-2.554
2	5	54.660	5.558	5	2	-53.445	-4.829	1.215	0.729
3	4	19.386	2.865	4	3	-19.346	-4.688	0.040	-1.823
4	5	6.598	0.518	5	4	-6.555	-5.171	0.043	-4.652
Total Loss								6.122	-10.777

3.2 Case 2: Newton-Raphson load flow carried out with the UPFC incorporated between buses 3 and 4 to control nodal voltage and increase active power flows. The result is depicted in Tables 3 and 4

Table 3. Bus Voltages With UPFC

Bus Voltage in Pu	Voltage Angle In Degree
1.0600	0.0000
1.0000	-1.7693
1.0000	-6.0161
0.9917	-3.1906
0.9745	-4.9741

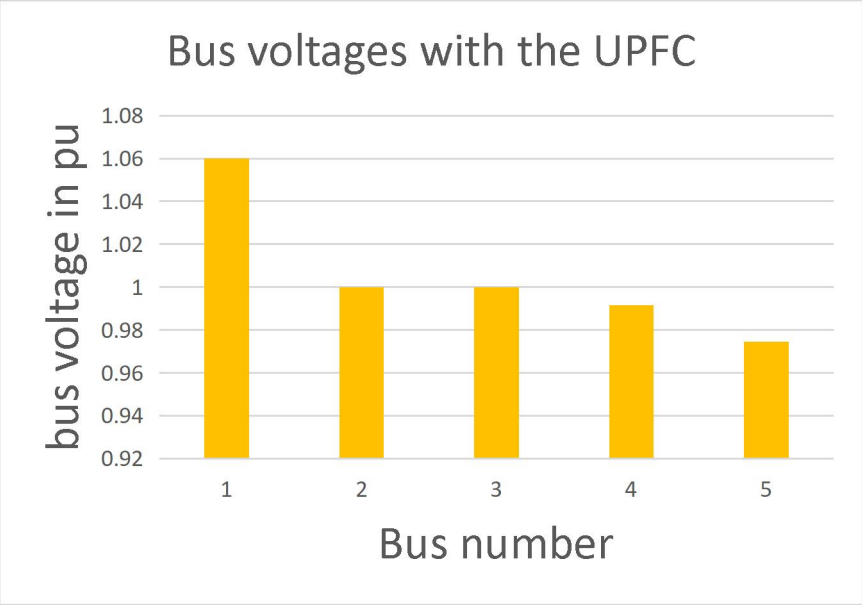

Figure 5: Voltages of the buses with the UPFC between buses 3 and 4

Table 4. Line Flows and Losses With UPFC

Line FLow and Losses

From Bus	To Bus	P MW	Q MVar	From Bus	To Bus	P MW	Q MVar	Line Loss MW	Line Loss MVar
1	2	81.143	76.424	2	1	-78.838	-75.879	2.305	0.545
1	3	50.341	9.343	3	1	-48.431	-8.924	1.909	0.419
2	3	37.484	-12.969	3	2	-36.569	11.715	0.915	-1.254
2	4	13.739	-1.780	4	2	-13.626	-1.847	0.113	-3.627
2	5	47.614	5.140	5	2	-46.690	-5.291	0.924	-0.151
3	4	40.000	2.000	4	3	-39.838	-3.490	0.162	-1.490
4	5	13.464	0.337	5	4	-13.310	-4.709	0.154	-4.371
Total Loss								6.484	-9.929

The power flows in the UPFC-upgraded network are different from the original situation, as was to be expected. The two most obvious differences are that bus 3 is receiving an additional 20% and 53% more active power from generator buses 1 and 2, respectively. The increase is a result of the UPFC series converter's high active power requirements.

The robustness of the UPFC shunt bus will determine the maximum amount of active power transferred between the UPFC and the AC system, 3. The generator at bus 1 reduces its reactive power generation by roughly 5.6% because the UPFC generates its own reactive power, and the generator linked at bus 2 increases its reactive power absorption by roughly 22.6%. Additionally, bus 3's nodal voltage magnitude is maintained at 1 p.u. by the UPFC shunt converter. It's important to remember that the UPFC keeps the active and reactive powers at 40MW and 2MVAR, respectively, when they leave the UPFC and head towards bus 3.

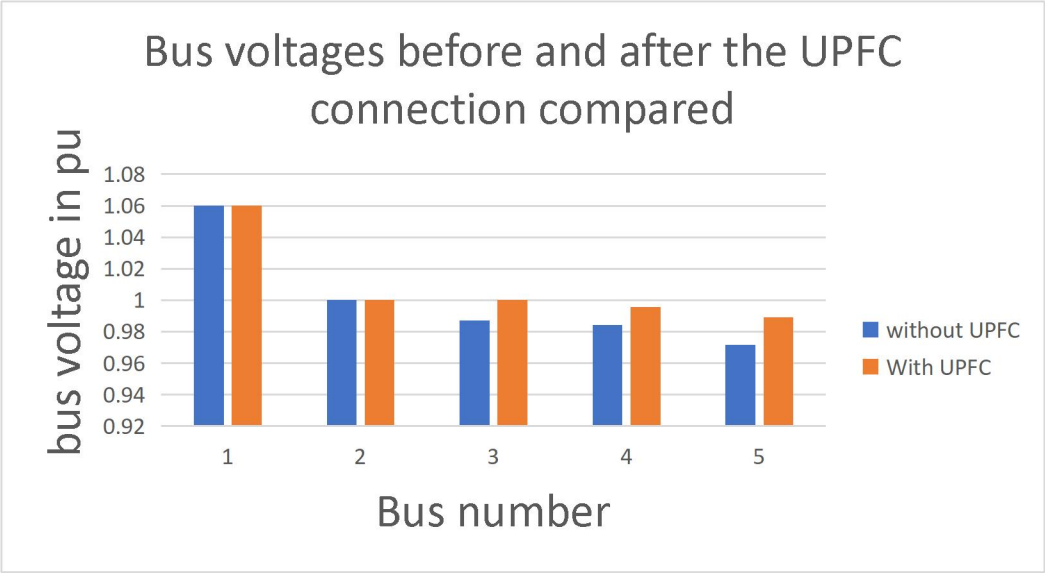

Figure 6: Voltages of the buses with and without the UPFC between buses 3 and 4

Table 6 Bus Data: IEEE 5 Bus System

Bus No	Bus Code	Voltage Magnitude	Angle	Load (MW)	Load (MVAR)	Gen (MW)	Gen (MVAR)	Qmin	Qmax
1	1	1.06	0	0.0	0.0	0.0	0.0	-500	500
2	2	1	0	20.0	10.0	40.0	0.0	-300	300
3	3	1	0	46.0	16.0	0.0	0.0	0	0
4	3	1	0	40.0	6.0	0.0	0.0	0	0
5	3	1	0	60.0	10.0	0.0	0.0	0	0

Table 7: Line Data for IEEE 5 Bus

From Bus	To Bus	R	X	B
1	2	0.02	0.06	0.06
1	3	0.08	0.24	0.05
2	3	0.06	0.18	0.04
2	4	0.06	0.18	0.04
2	5	0.04	0.12	0.03
3	4	0.01	0.03	0.02
3	5	0.08	0.24	0.05

Conclusion

This paper concentrated on reactive power compensation and the use of UPFCs to boost active power flows in transmission lines. The power-flow problem has been solved using the Newton-Raphson load flow method. A modified UPLC power flow model was used to investigate the impact of UPFC on the power system. The modified load flow program was utilized to access the impact of UPFC on the system, and UPLC was positioned between buses 3 and 4.

In MATLAB, the simulation was carried out. Plots were used to depict the findings of a load flow analysis conducted on a five-bus system, which revealed that the voltage profile of the system had improved. Additionally, it was clear that the UPFC was positioned at a bus where the voltage magnitude was kept at one p.u.

Based on the data, it can be said that the UPFC has the greatest influence on voltage compensation and that power flows to the bus closest to it, with its impact decreasing with increasing distance from the bus.

References

Asha, K., Manjula, M., Sarma, V.R. (2021). Mitigation of Various Power Quality Problems Using Unified Series Shunt Compensator in PSCAD/EMTDC. *16th National Power Systems Conference*, 100-105.

Bhowmik, A. and Nandi, C., (2019). Implementation of Unified Power Flow Controller (UPFC) for Power Quality Improvement in IEEE 14-Bus System. *International Journal of Computer Technology and Application,* 2 (6),1889-1896.

Gaurav, N. and Saxena, N. (2018). Power Quality improvement using UPFC. *International Journal of Electrical, Electronics and Computer Engineering*, 2(2),30- 33.

Gopinath, N., Vinothini, A., Kumar, S.(2014). Modeling of UPFC Using Model Predictive Control and Bacterial Foraging Algorithm. *International Journal of Innovative Research in Computer and Communication Engineering*, 2(1), 2724-2731.

Jiang, X. Chow, J.H., Edris, A., Fardanesh, B., Uzunovic, E. (2010). Transfer path stability enhancement by voltage-sourced converter-based FACTS controllers. *IEEE Transactions on Power Delivery*, 25(3), 1019-1025.

Khonde, S., Dhamse S., Thosar, A.G. (2020). Power Quality Enhancement of Standard IEEE 14 Bus System using Unified Power Flow Controller. *International Journal of Engineering Science and Innovative Technology (IJESIT)*, 3(5), 323-334.

Lakshmi, N., Sravanthi, G., Ramadevi, L., Chowdary, K.H. (2015). Power quality and stability improvement of HVDC transmission System using UPFC for Different uncertainty conditions. *International Journal of Scientific & Engineering Research*, 6(2), 795-801.

Mathad,V., Basanagouda, F. R., Jangamshetti, S. H., (2018). Voltage Control and Power System Stability Enhancement using UPFC. *International Conference on Renewable Energies and Power Quality (ICREPQ'14)*, 1(12), 871-875.

Mohanty, A., Ahamad, M., Khan, M.A., (2023). Modeling, Simulation and Performance Analysis of FACTS Controller in Transmission line. *International Journal of Emerging Technology and Advanced Engineering,* 3(5), 429-435.

Nwaorgu, O. A., Ifeagwu, N.E**.** Udo, E.U. (2016). Cost Analysis of Power Outages in Nigerian University. A case study of Michael Okpara University of Agriculture*. Umudike.* Umudike *Journal of Engineering and Technology (UJET),* 1(2), 85-92.

Oputa, O., Diyoke, G. C., Ifeagwu, E. N. (2017). Power Flow Analysis of Electric Transmission System In the Southern Nigeria*. Umudike.* Umudike *Journal of Engineering and Technology (UJET),* 2(1), 153-160.

Rai, A. (2018).Enhancement of Voltage Stability and reactive Power Control of Distribution System Using Facts Devices. *International Journal of Scientific Research Engineering and Technology,* 1(9), 001-005.

Sindekar, A. and Parate, J. (2012). Reactive Power Control and Transmission loss reduction with realization of SVC and TCSC. (Electronic version). *International Journal of Engineering Science and Technology.* 4 (7), 3592 – 3600

Singh, B. (2010). Incorporation of FACTS Controllers in Newton Raphson Load Flow for Power Flow Operation, Control and Planning: A Comprehensive Survey. (Electronic version). *International Journal on Computer Science and Engineering.* 2 (6), 2117- 2124

Soruban, J D., Sathyaraj, A., Gnana Chandran, J.J.,(2020). Power Quality Enhancement Using UPFC as an Active Power Filter for Renewable Power Generation. *International Journal of Advanced Research in Electrical, Electronics and Instrumentation Engineering*, 4(3),1712-1718.

Vaibhav, K., Prashant, P. Khatri, R.(2013).Unified Power Flow Controller for Power Quality Improvement. *International Journal of Emerging Science and Engineering (IJESE),* 1(10),1-4.

Zhang, C., Rehtanz, A., Pal, B.(2018). FACTS-Devices and Applications in Flexible AC Transmission Systems: *Modelling and Control, ed: Springer*, 1-30.